

Post-quench Ductility Results for North Anna High-burnup 17×17 ZIRLO Cladding with Intermediate Hydrogen Content

Y. Yan, T. A. Burtseva, and M. C. Billone
Argonne National Laboratory
April 17, 2009

1. Pre-test characterization

Figure 1 shows the axial locations of North Anna ZIRLO Rod AM2-L17 from which Studsvik sectioned and defueled 80-mm-long cladding segments for ANL. Segment axial orientation relative to the bottom of the fuel rod was not maintained during defueling. Characterization results for LOCA pre-test planning were generated for samples sectioned from segments labeled 1 and 2 in Fig. 1, which correspond to ANL identification numbers 648A and 648B, respectively.

Figure 2 shows micrographs at one of eight circumferential locations for: (a) cladding cross section; (b) corrosion layer; and (c) fuel-cladding bond. The measured thicknesses were 26 ± 1 μm for the corrosion layer, 551 ± 5 μm for the metal wall, and $\approx 7\pm 1$ μm for the fuel-cladding bond. However, as shown in Fig. 1c, local regions of the bond layer were about 20-25 μm thick. These thicker bond regions are consistent with the higher (factor of 2) gamma dose-rate readings for 648A and 648B, as compared to the dose rate reading for 648F (segment 6 in Fig. 1).

Figure 3 shows the hydride morphology at two circumferential locations adjacent to the sample with 318 ± 30 wppm of hydrogen in the corroded cladding. As is typical of seven of the eight locations imaged, the hydrides are primarily circumferential and clustered in a dense rim near the corrosion layer, as is shown in Fig. 3a. Figure 3b shows one location that had long radial hydrides within the inner third of the cladding wall. For LOCA events, the radial variation in hydrogen content and hydride morphology are not important because hydrogen homogenizes quickly across the beta phase of the cladding.

Table 1 summarizes the characterization results for corrosion-layer thickness, cladding-metal thickness, fuel-cladding-bond layer thickness, and LECO-measured hydrogen content. For LECO measurements, short cladding rings (≈ 2 -mm-long) were sectioned and then snipped into four quarter rings. The hydrogen content and mass were measured for each quarter ring. The hydrogen content included the hydrogen evolved from the cladding metal and the corrosion layer, as well as the bond layer. The mass included the masses of the corrosion layer, the cladding metal, and the fuel-cladding bond. The four measurements per ring were also used to determine the one-sigma ($1-\sigma$) circumferential variation in hydrogen content. Based on the data listed in Table 1, the weight-averaged hydrogen contents of the two segments are 310 ± 32 wppm for 648A and 366 ± 30 wppm for 648B. Two LOCA oxidation samples were sectioned from 648A, and three LOCA oxidation samples were sectioned from 648B.

The pre-test hydrogen data were used for choosing target oxidation levels (i.e., CP-ECR values). However, it was also realized that the hydrogen content in the cladding metal could be higher or lower than what was measured. As documented in Appendix A, LOCA samples were weighed before and after oxidation tests. Post-LOCA hydrogen contents were corrected for weight gain (1-2%). A final correction was made to take into account the ratio of the pre-test sample mass (measured) and metal mass (calculated from metallographic results). This factor (1.06 to 1.10) varied from sample to sample and reflected the added weight of the pre-test sample due to the fuel-cladding bond, which included fission products and actinides (heavier than Zr) in or adherent to the fuel-cladding bond. As shown in Table 1, the pre-test hydrogen in the metal is close to what was measured for the pre-test corroded samples.

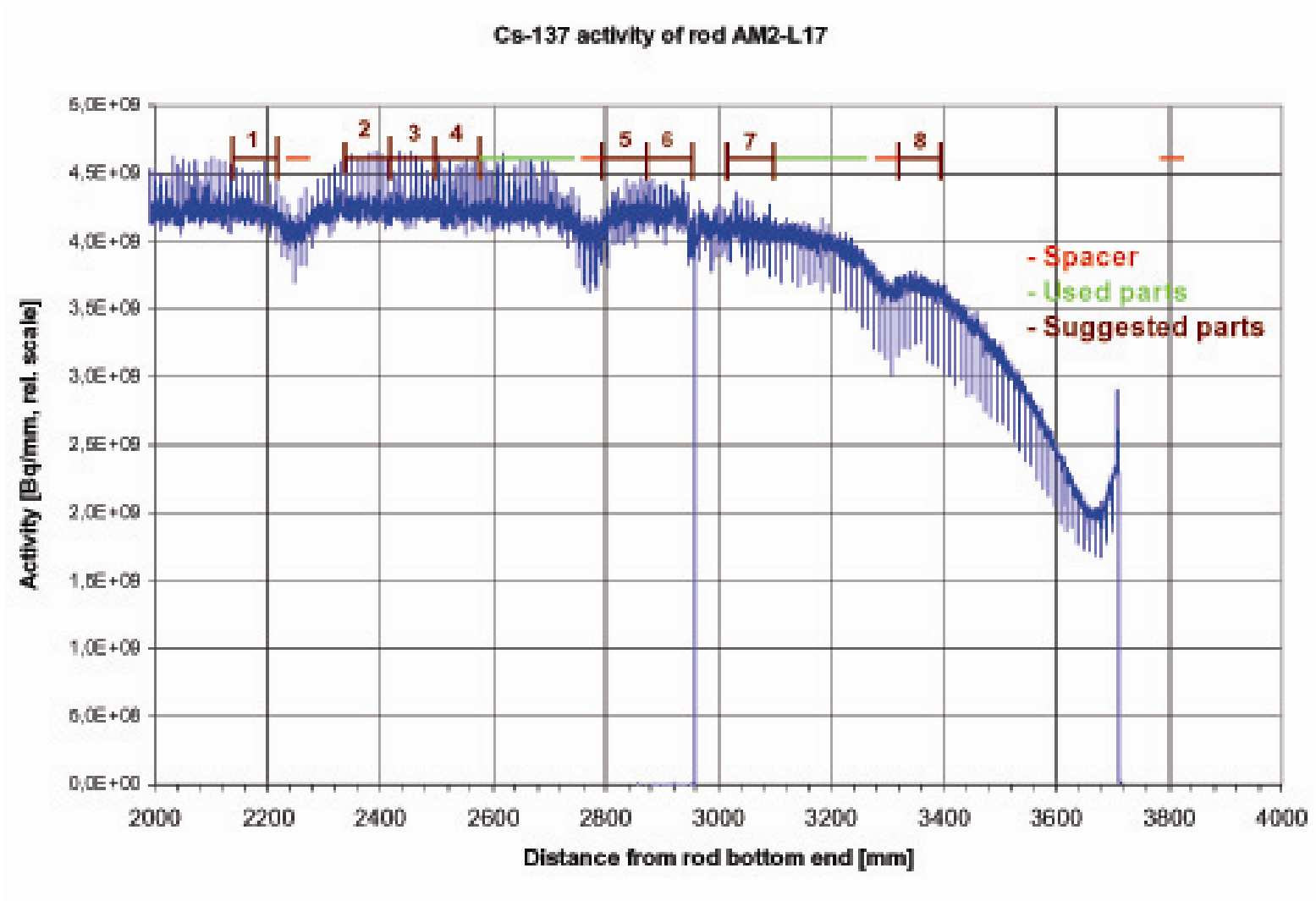
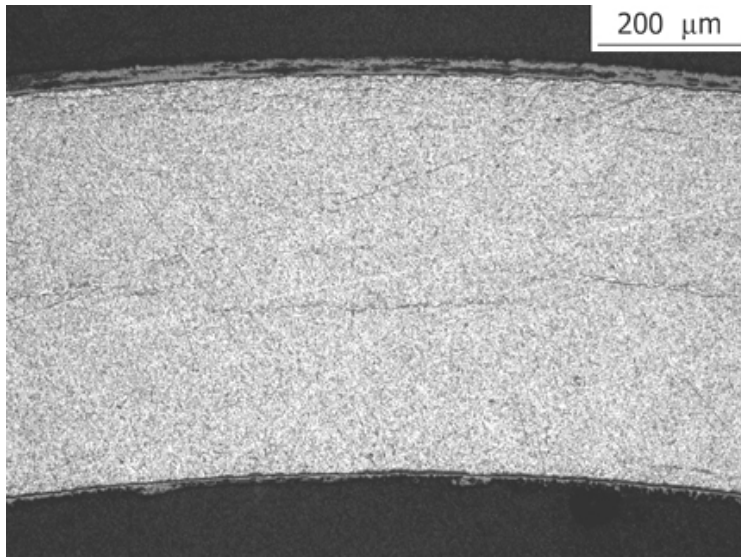
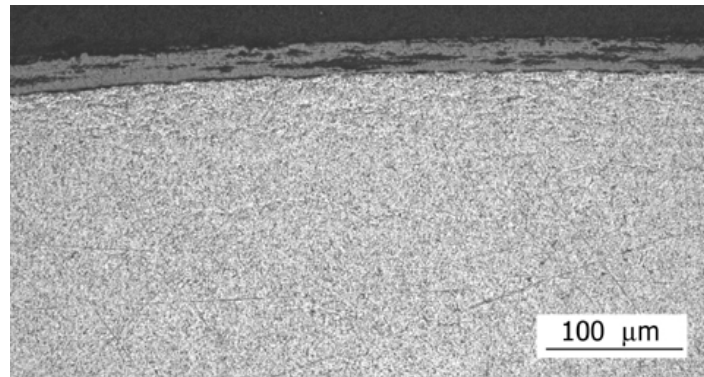


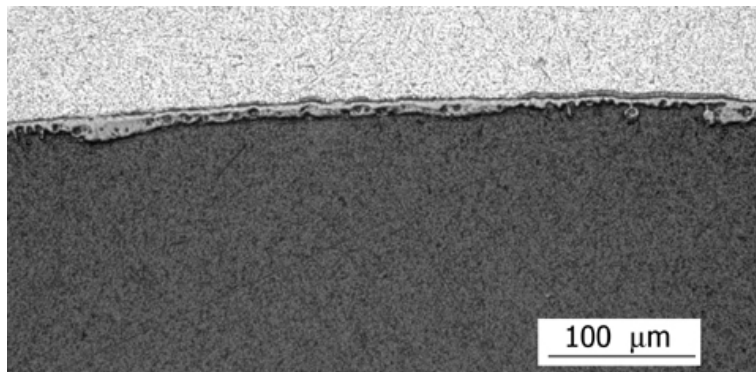
Fig. 1. Sectioning diagram for North Anna ZIRLO defueled cladding segments sent to ANL from Studsvik in second shipment. Corresponding ANL ID numbers are 648A and 648B for segments 1 and 2, respectively (from Ref. 1).



(a) Cladding cross section

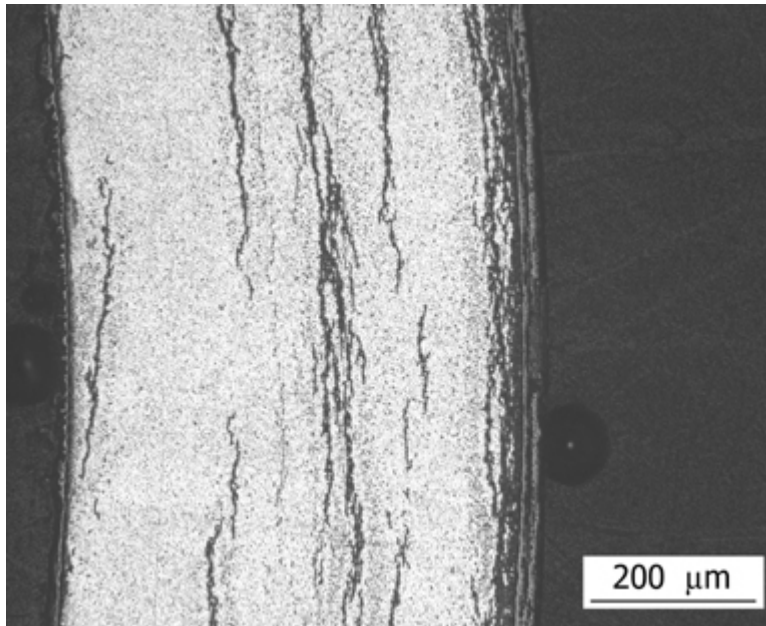


(b) Corrosion layer

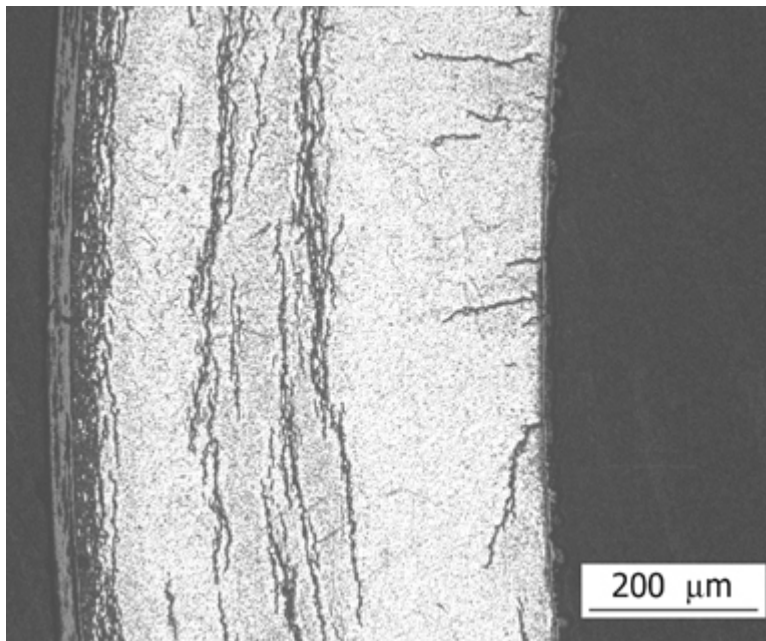


(c) Fuel-cladding bond layer

Fig. 2. Micrographs taken from a sample sectioned near the middle of segment 648A: (a) cladding cross section; (b) corrosion layer; and (c) fuel-cladding bond.



(a) Circumferential hydrides



(b) Circumferential and radial hydrides

Fig. 3. Hydride morphology for 648A sample with 318 ± 30 wppm hydrogen: (a) circumferential hydrides (typical); and (b) circumferential and radial hydrides (one of eight locations).

Table 1. North Anna ZIRLO Characterization Results for Rod AM2-L17

Sample ID # W (ANL)	Corrosion Layer from Eddy Cur. (EC), μm	Corrosion Layer from Metallography, μm	Metal Layer from Metallography, μm	Fuel-Clad Bond Layer from Met., μm	Hydrogen in Corroded Cladding, wppm	Hydrogen in Cladding Metal, wppm
1 (648A)	25-28	---	---	---	294 \pm 29	296 \pm 33
		26 \pm 1	551 \pm 5	7 \pm 1 ^a	318 \pm 30	
		---	---	---	317 \pm 38	
2 (648B)	25-30	---	---	---	361 \pm 36	340 \pm 34
		---	---	---	367 \pm 29	
		---	---	---	370 \pm 33	

^aLocal regions of bond layer were as thick as 20-25 μm .

2. Thermal and Metallurgical Benchmark Tests for Bare and Oxidized ZIRLO

Thermal benchmark tests were conducted in the out-of-cell LOCA apparatus with two thermocouples (TCs) welded onto fresh (as-fabricated) ZIRLO samples, in addition to the three TCs permanently welded to the Inconel holder just above the sample. Tests were repeated with fresh samples until furnace control parameters were established to give the desired temperature ramp and hold temperature. The results of benchmark test ZLU#145 with a bare ZIRLO sample are shown in Fig. 4. The time for the sample to reach 1200°C was about 100 s. At 150 s, the average of the two sample TCs was 1202 \pm 7°C. The heating phase of the test was 200 s. The corresponding CP weight gain and CP-ECR, including the cooling phase, were 8.27 mg/cm² and 12.7%, respectively. The CP-calculated oxide layer grown on the inner and outer surfaces of the cladding was about 40- μm thick.

For high-burnup ZIRLO cladding, the corrosion and bond oxide layers will result in a slower ramp rate compared to the rate for bare ZIRLO. At the completion of benchmark test ZLU#145, the oxidized sample was again ramped to temperature using the same control parameters as were used for ZLU#145. To distinguish these two tests, the one with the pre-oxidized sample was called ZLU#145A. Figure 5 shows the comparison between the average cladding temperatures for bare and pre-oxidized ZIRLO. The small temperature pre-peak was reduced from \approx 1110°C to 1060°C. The average ramp rates to 1200°C were comparable. However, the time to reach 1200°C was longer for the pre-oxidized cladding (150 s vs. 100 s for bare cladding). The average temperature of the pre-oxidized cladding was 1200 \pm 3°C at 150 s during the heating phase. It was later verified that there was essentially no difference in the thermal response of pre-oxidized cladding samples with thin (\approx 12 μm) and thick (\approx 40 μm) oxide layers. Thus, the ZL#145A thermal history was determined to be appropriate one for high-burnup cladding LOCA tests.

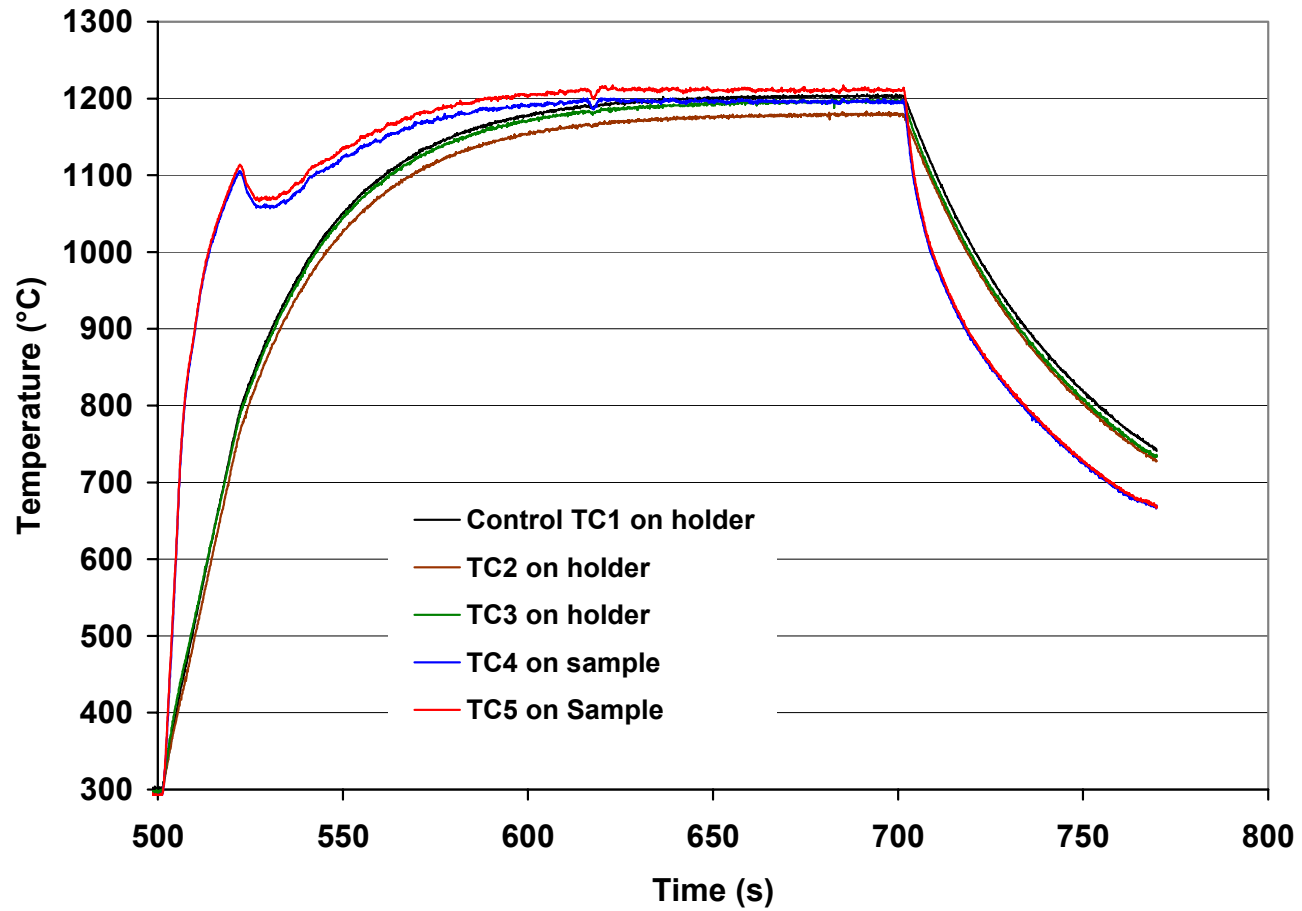


Fig. 4. Thermal history for bare ZIRLO cladding determined from test ZLU#145. At 150 s into the heating phase, the average sample temperature was $1202 \pm 7^\circ\text{C}$.

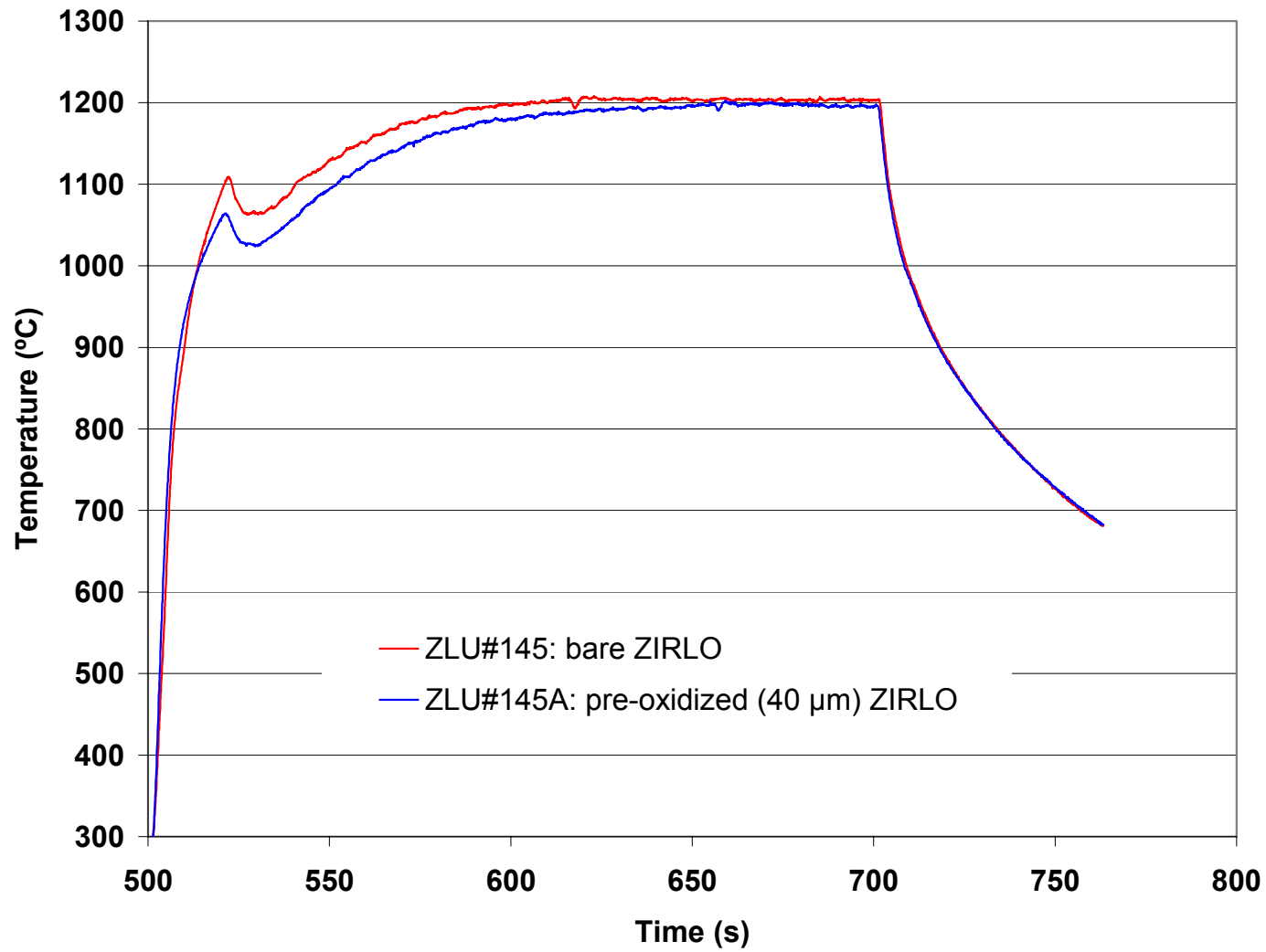


Fig. 5. Thermal history for bare ZIRLO (ZLU#145) and pre-oxidized (ZLU#145A) cladding. At 150 s into the heating phase, the average temperature for the pre-oxidized sample was $1200 \pm 3^\circ\text{C}$.

The test train benchmarked in the out-of-cell LOCA apparatus, located just outside the hot cell, was installed into the in-cell apparatus located in Cell #4 of the Irradiated Materials Laboratory (IML) with the same three holder TCs welded onto the sample holder. A weight-gain benchmark test was conducted in-cell with bare ZIRLO. The same temperature history and heating-phase shown in Fig. 4 were used to conduct the weight-gain benchmark test ZLU#146. The measured weight gain (7.91 mg/cm²) was within 5% of the CP-calculated weight gain (8.27 mg/cm²). The CP-calculated weight gain was based on the ZLU#145 results. These results validate the use of the ZLU#145A thermal history for in-cell tests with corroded high-burnup ZIRLO samples.

3. Ductility Results for High-burnup North Anna ZIRLO

Four LOCA oxidation tests and 9 ring-compression ductility tests were conducted with samples sectioned from high-burnup ZIRLO segments 648A and 648B. Characterization results for these segments are given in Table 1. Post-oxidation and post-quench-ductility (PQD) data are summarized in Table 2.

For test planning purposes, the measured cladding wall thickness (0.55 mm) was used to derive the relationship between CP-ECR (in %) and Wg (in mg/cm²):

$$\text{CP-ECR} = 1.594 \text{ Wg} \quad (1)$$

Test ZLI#7 was conducted without quench with a sample containing about 340 wppm hydrogen in the cladding metal to ensure adequate ductility at 10% CP-ECR. The heating-phase test time (153 s) and corresponding CP-ECR (10%) are shown in Fig. 6 (see ZLU#145A history in Fig. 5). The pre-test sample outer diameter was 9.50 mm. Subtracting off the corrosion layer thickness measured at a neighboring location gave a pre-test cladding-metal outer diameter of about 9.45 mm. This pre-test metal diameter was used to normalize offset and permanent displacements to determine offset and permanent strains. As shown in Table 2, the offset and permanent strains at 135°C were in the range of 10-13% and 5-9%, respectively. These results indicate significant ductility for the slow-cooled LOCA sample following oxidation to 10% CP-ECR. The results were used to plan the first test with quench.

For test ZLI#8, a lower hydrogen content (\approx 300 wppm) sample from 648A was used. The test time and CP-ECR were kept the same as were used for test ZLI#7. However, the sample was quenched at 800°C. The effects of quench were significant in that the rings sectioned from the LOCA sample were brittle even though the sample had less hydrogen in the metal than the ZLI#7 sample. The offset strains were 0.7% (brittle) and 2.2% (borderline ductile), which imply brittle behavior based on the offset strain criterion documented in Ref. 2. Permanent displacements and strains could not be determined because the rings cracked into two pieces.

In order to bracket the ductile-to-brittle transition oxidation level, test ZLI#9, also with \approx 300 wppm hydrogen, was conducted for a heating-phase time of 118 s, which corresponded to 8% CP-ECR. As shown in Fig. 6, the peak oxidation temperature at the end of the heating phase was 1190°C. The first two rings compressed at 135°C also cracked at top and bottom locations with adequate offset strains of 2.9% and 4.6% indicative of ductile behavior. In order to confirm the ductile behavior, it was necessary to terminate the loading for the third ring before cracking occurred and after sufficient offset strain (\geq 2%). Although there was a very low probability of achieving these goals, the test was successful in that the offset and permanent displacements of the uncracked ring were determined to be 0.19 mm and 0.11 mm, respectively. These correspond to 2.0% offset and 1.2% permanent strains (see Fig. B7 in Appendix B).

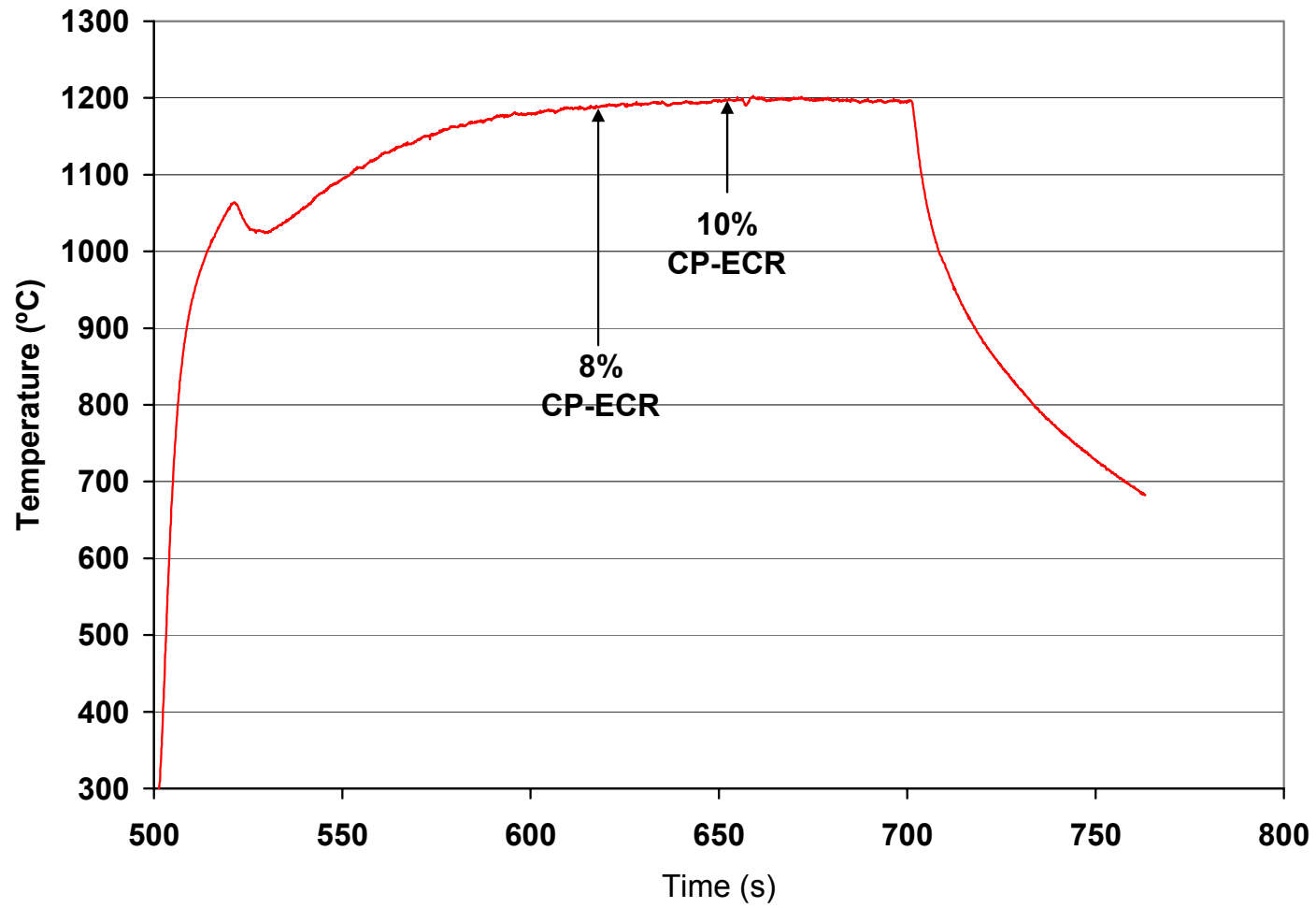


Fig. 6. Thermal history and test times for high-burnup ZIRLO tests conducted to 8% (ZLI#9 and ZLI#11) and 10% (ZLI#7-8) CP-ECR.

Table 2. Post-Test Ductility Results for High-Burnup North Anna ZIRLO Cladding Oxidized at $\leq 1200^{\circ}\text{C}$, Cooled with or without (ZLI#7) Quench at 800°C , and Ring-Compressed at 135°C ; SC= slow cooled without quench

Test #	Pre-test Hydrogen Content, wppm		Test Time, ^b s	Peak Temperature, $^{\circ}\text{C}$	CP-ECR, %	Strain, %	
	Cladding	Metal ^a				Offset ^c	Permanent
ZLI#7 SC	366 \pm 30 for 0.53-g sample	340 \pm 34 for 0.28-g sample	153	1200	10	9.9 13.4	5.0 9.4
ZLI#8 Quench at 800°C	310 \pm 32 for 0.53-g sample	294 \pm 37 for 0.76-g sample	153	1200	10	0.7 2.2	--- ---
ZLI#9 Quench at 800°C	310 \pm 32 for 0.53-g sample	296 \pm 35 0.72-g sample	118	1190	8	2.9 4.6 >2.0	--- --- >1.2
ZLI#11 Quench at 800°C	366 \pm 30 for 0.53-g sample	340 \pm 34 for 0.28-g sample	118	1190	8	0.6 1.0	--- ---

^aSee Appendix A for determination of pre-test hydrogen content in cladding metal.

^bFrom beginning of ramp at 300°C to end of heating phase.

^cSee Appendix B for load-displacement curves.

Based on the results in Table 2 for tests ZLI#8 and ZLI#9, the ductile-to-brittle transition oxidation level is 9% CP-ECR for 300-wppm pre-test hydrogen content in the metal. Following this determination, the remaining two LOCA samples with 340-wppm pre-test hydrogen content in the metal were used for PQD tests. During the ZLI#10 ramp, the control thermocouple failed and the test was terminated after the other two thermocouples on the holder recorded temperatures above 1250°C. The remaining sample was oxidized to 8% CP-ECR in test ZLI#11 and quenched at 800°C. As indicated in Table 2, the two rings sectioned from this LOCA sample had very low offset strains (0.6-1.0%) indicating embrittlement. Although the ductile-to-brittle transition CP-ECR could not be determined precisely, the data point is useful in establishing that the transition CP-ECR is < 8% for 340-wppm hydrogen.

4. Discussion

The embrittlement results for high-burnup 17×17 ZIRLO with 300-wppm pre-test hydrogen are consistent with the results presented in Ref. 1 for prehydrided (pre-H) 17×17 Zry-4. At 10% CP-ECR with quench at 800°C, pre-H 17×17 Zry-4 had low ductility (2.8% offset strain) with 274-wppm hydrogen and was brittle with 335-wppm hydrogen. Although the ductile-to-brittle transition hydrogen content was given in Ref. 1 as 300±25 wppm for 10% CP-ECR, it is more likely that the transition occurs in the narrower range of 290±10 wppm. High-burnup ZIRLO with 300-wppm hydrogen had an embrittlement threshold of 9% CP-ECR. Based on the uncertainties in testing high-burnup cladding and the limited database for prehydrided cladding, results for both materials might overlap if multiple tests were conducted in the range of 8-10% CP-ECR for cladding with 300-wppm hydrogen. However, the prehydrided Zry-4 samples were subjected to faster temperature ramps and had slightly thicker cladding metal (0.57-mm) than the high-burnup samples (0.55 mm). Thus, for the same CP-ECR level, prehydrided Zry-4 samples were exposed to longer times at 1200°C than high-burnup ZIRLO samples. A better comparison could be made if prehydrided ZIRLO with 300-wppm hydrogen were tested in the same test train with a similar temperature ramp rate as the one used for the high-burnup ZIRLO tests.

Also given in Ref. 1 are ductility data for prehydrided 17×17 Zry-4 and 15×15 Zry-4 oxidized to a heating-phase CP-ECR of 7.5% and quenched at 800°C. The total CP-ECR for these samples, including the small weight gain during cooling, was 7.9% and 7.7%, which can be rounded off to 8%. For 17×17 Zry-4, the embrittlement hydrogen content was <400 wppm. For 15×15 Zry-4, the embrittlement hydrogen content was >360 wppm and <390 wppm. Although the embrittlement hydrogen content was given in Ref. 1 as 375±25 wppm, it is more likely that it occurs in the narrower range of 375±15 wppm. Thus, the data point for high burnup ZIRLO with 340-wppm hydrogen was expected to be borderline ductile at 8% CP-ECR, especially as the peak oxidation temperature was slightly less than 1200°C. It appears likely that high-burnup ZIRLO with 340-wppm would have been ductile at 7% CP-ECR.

The new results for PQD embrittlement threshold are compared to the ductility results presented in Ref. 1 for as-fabricated, prehydrided and high-burnup cladding materials. The ductility criteria used to determine the ductile-to-brittle threshold are those documented in Ref. 2: the highest CP-ECR rounded to the nearest percent for which the average permanent strain is $\geq 1\%$ or the one-sigma ($1-\sigma$) lower-bound offset strain is $\geq 1.60 + 0.0534 \text{ CP-ECR (in \%)}$ if the permanent strain cannot be determined. Note that in Ref. 1 the one-sigma lower-bound permanent strain, not the average, was required to be $\geq 1\%$. Table 3 gives the recalculated results for as-fabricated cladding materials. Table 4 gives the results for prehydrided and high-burnup cladding materials. The last column, "Comments", in both tables indicates how the embrittlement thresholds were determined. The hydrogen contents for high-burnup ZIRLO and M5 have been corrected to reflect the pre-test hydrogen content in the metal (see Appendix A).

Table 3. Embrittlement Oxidation Level for As-fabricated Cladding Alloys Oxidized at 1200°C and Quenched at 800°C; ductility criteria documented in Ref. 2 were used to determine ductile-to-brittle transition CP-ECR (to nearest percent): average permanent strain \geq 1% or one-sigma lower-bound offset strain \geq 1.60 + 0.0534 CP-ECR

12

Material	Pre-test Hydrogen Content, wppm		Peak T, °C	CP-ECR, %	Strain, %		Comment
	Cladding	Metal			Offset	Permanent	
17×17 M5	5	5	1200	20	3.5±0.5	1.0	Embrittlement threshold based on average permanent strain for 2 ring tests
15×15 Zry-4	26	26	1200	20	2.4±0.4	1.1±0.4	Embrittlement threshold based on average permanent strain for 2 ring tests
17×17 ZIRLO	5	5	1200	19	2.6±0.8	1.1±0.2	Embrittlement threshold based on average permanent strain for 2 ring tests
10×10 Zry-2	13	13	1200	20	1.7±0.3	1.0±0.1	Embrittlement threshold based on average permanent strain for 2 ring tests
17×17 Zry-4	5	5	1200	19	2.6±0.8	1.1±0.2	Embrittlement threshold based on average permanent strain for 2 ring tests
15×15 Zry-4 HBR-type	22	22	1200	16	2.9±0.5	1.1±0.3	Embrittlement threshold based on average permanent strain for 7 ring tests

Table 4. Embrittlement Oxidation Level as a Function of Pre-test Hydrogen Content for Prehydrided and High-burnup Cladding Materials Oxidized at $\leq 1200^{\circ}\text{C}$ and Quenched at 800°C ; ductility criteria documented in Ref. 2 were used to determine ductile-to-brittle transition CP-ECR (to nearest percent): average permanent strain $\geq 1\%$ or one-sigma lower-bound offset strain $\geq 1.60 + 0.0534$ CP-ECR

Material	Pre-test Hydrogen Content, wppm		Peak T, $^{\circ}\text{C}$	CP-ECR, %	Strain, %		Comment
	Cladding (mass)	Metal (mass)			Offset	Permanent	
Ringhals High-burnup 17x17 M5	108 \pm 10 (0.40 g)	137 \pm 16 (1.56 g)	1200	15.1 13.4	2.8 \pm 0.7 4.2 \pm 0.2 (or 3.4 \pm 1.3)	--- ---	Recommend 14 \pm 1% CP-ECR for embrittlement; see text on p. 14 for explanation
17x17 Zry-4 Prehydrided	290	290	1200	10	2.1%	--	Extrapolation of data for 209- and 274-wppm H rings gives 2.1% offset at 290 wppm
NA High-burnup 17x17 ZIRLO	310 \pm 32 (0.53 g)	296 \pm 33 (1.44 g)	1200 1190	10 8	1.5 \pm 1.1 3.8 \pm 1.2	--- >1.2	Recommend 9% CP-ECR based on 1 ductile ring at 10% and 3 at 8%
HBR-type 15x15 Zry-4 Prehydrided	360 386	360 386	1200 1200	8 8	5.0 1.2 \pm 0.7	--- 0.5 \pm 0.2	Interpolation gives 1- σ lower bound of 2.0% offset strain at 377 wppm, which is rounded down to 370 wppm
HBR-type 15x15 Zry-4 Prehydrided	\approx 530	\approx 530	1190	5	\approx 2	---	Based on extrapolation of data for 460-520 wppm hydrogen samples
HBR High-burnup 15x15 Zry-4	550 \pm 100 (1.52 g)	\approx 550 \pm 100 (1.52 g)	1180	5	---	---	Based on 37% offset stain for 4.5% CP-ECR sample cooled without quench
NA High-burnup 17x17 ZIRLO	620 \pm 140 (0.55 g)	540 \pm 114 (0.26-g) 592 \pm 115 (0.27-g)	1176 1132	6.3 4.0	0.8 \pm 0.5 >43	0.2 >43	Based on interpolation, transition is at 5% CP-ECR for 540 \pm 114 wppm with 1162 $^{\circ}\text{C}$ peak cladding T

For as-fabricated (AF) cladding materials, determination of the ductile-to-brittle transition CP-ECR was straightforward as permanent displacements and strains were measured for the rings, which exhibited single, tight through-wall cracks. For prehydrided (PH) Zry-4, the tests were conducted at fixed oxidation levels with samples containing varying amounts of hydrogen. For early tests, samples had significant axial variation in hydrogen content (e.g., all 17×17 Zry-4 and some HBR-type 15×15 Zry-4). For later tests with HBR-type 15×15 Zry-4, the hydrogen content was relatively uniform. In determining the ductile-to-brittle hydrogen content for PF Zry-4 at 5% and 8% CP-ECR, data from samples with uniform hydrogen content were primarily used. However, reliance on the offset strain ductility criterion leads to added uncertainty in determining the embrittlement hydrogen content.

The data for high-burnup ZIRLO were relatively straightforward even though many of the rings failed with two cracks. However, by terminating one of the tests prior to failure, it was established at 8% CP-ECR that 2.0% offset strain corresponded to 1.2% permanent strain. Although the embrittlement thresholds were determined using offset strains, there is a relatively high confidence in the offset strain ductility criterion for high-burnup ZIRLO at oxidation levels $\leq 10\%$ CP-ECR. In addition, the rapid decrease in both offset and permanent strains in the range of 4-6% CP-ECR for high-burnup ZIRLO with ≥ 540 -wppm hydrogen resulted in a straightforward interpolation of 5% CP-ECR embrittlement threshold.

The data for high-burnup M5 are important because of the low hydrogen content. These data were also the most difficult to assess because all of the rings from quenched LOCA samples failed with two cracks, rendering it impossible to measure permanent strain. Also, the decrease in offset strain with increasing CP-ECR was very gradual: $3.4 \pm 1.3\%$ (or $4.2 \pm 0.02\%$ for 2 of the 3 rings) at 13.4% CP-ECR, $2.8 \pm 0.7\%$ at 15.1% CP-ECR, and $2.9 \pm 0.12\%$ for 16.1% CP-ECR. The 1- σ lower-bound offset strains are: 2.1% (or 4.0% for 2 of the 3 rings), 2.1%, and 1.7%, for 13.4%, 15.1%, and 16.1% CP-ECR, respectively. The corresponding offset-strain ductility limits are: 2.3% at 13.4% CP-ECR, 2.4% at 15.1% CP-ECR and 2.5% at 16.1% CP-ECR. Using these limits would imply that high-burnup M5 would be brittle for $\geq 13.4\%$ CP-ECR and perhaps ductile at 13% CP-ECR. However, excluding the one low ring-compression data point (1.9% offset strain) for the 13.4% CP-ECR sample would give a 1- σ lower-bound offset strain of 4.0% at 13.4% CP-ECR. Based on linear interpolation, the ductile-to-brittle transition CP-ECR would be 14.8%. Thus, within the uncertainty of the database and data assessment, the transition CP-ECR listed in Table 4 for high-burnup M5 is $14 \pm 1\%$.

The high-burnup M5 test samples for LOCA PQD tests at 15.1% CP-ECR (645C3) and 13.4% CP-ECR (645C6) were sectioned from an 80-mm-long segment (645C), which was wire-brushed to partially remove fuel-cladding bond material in order to reduce the gamma and beta-gamma dose rates of the material. Based on gamma dose-rate reduction after wire-brushing, it was clear that about half of the gamma-emitting isotopes (e.g., Ru-106, Sb-125, Cs-134, Cs-137, and Eu-154) were mechanically removed. Along with these isotopes, it is probable that actinides (alpha, beta, and gamma emitters) were also partially removed. Metallography was performed at a location between the two LOCA samples to confirm that the 8- μm fuel-cladding bond layer was intact. It exhibited a more uniform fuel-side surface indicating that the wire-brushing removed fingers and thinned local regions of increased bond thickness.

The embrittlement data contained in Tables 3 and 4 are summarized in Table 5 for ductile-to-brittle oxidation level vs. hydrogen content. Based on uncertainty and circumferential variation, average values listed in Table 5 are rounded to the nearest 10 wppm for hydrogen and 10°C for temperature. Also included in Table 5 are high-burnup data for CP-ECR values that are greater or less than the embrittlement threshold. These were used as a guide in establishing the relationship between embrittlement threshold and hydrogen content. The data for embrittlement oxidation level vs. pre-test hydrogen content in the metal are plotted in Fig. 7.

Table 5 Summary of Ductile-to-brittle transition oxidation level (embrittlement CP-ECR) vs. pre-test hydrogen content in cladding metal for As-fabricated (AF), Prehydrided (PH) and High-burnup Cladding Materials; NA = North Anna and HBR = H. B. Robinson

Cladding Material	Pre-test Hydrogen Content in Cladding Metal, wppm	Peak Oxidation Temperature, °C	Embrittlement CP-ECR, %
AF 17×17 M5	5	1200	20
AF 15×15 Zry-4	26	1200	20
AF 17×17 ZIRLO	5	1200	19
AF 10×10 Zry-2	13	1200	20
AF 17×17 Zry-4	5	1200	19
AF HBR-type 15×15 Zry-4 (Old Vintage Cladding)	22	1200	16
Ringhals High-burnup 17×17 M5	140	1200	14±1
PH 17×17 Zry-4	290	1200	10
NA High-burnup 17×17 ZIRLO	300	1200	9
NA High-burnup 17×17 ZIRLO	340	1180	<8
PH HBR-type 15×15 Zry-4	370	1200	8
NA High-burnup 17×17 ZIRLO	450	1160	>5
PH HBR-type 15×15 Zry-4	530	1190	5
HBR High-burnup 15×15 Zry-4	550	1190	5
NA High-burnup 17×17 ZIRLO	540	1160	5
NA High-burnup 17×17 ZIRLO	590	1130	>4

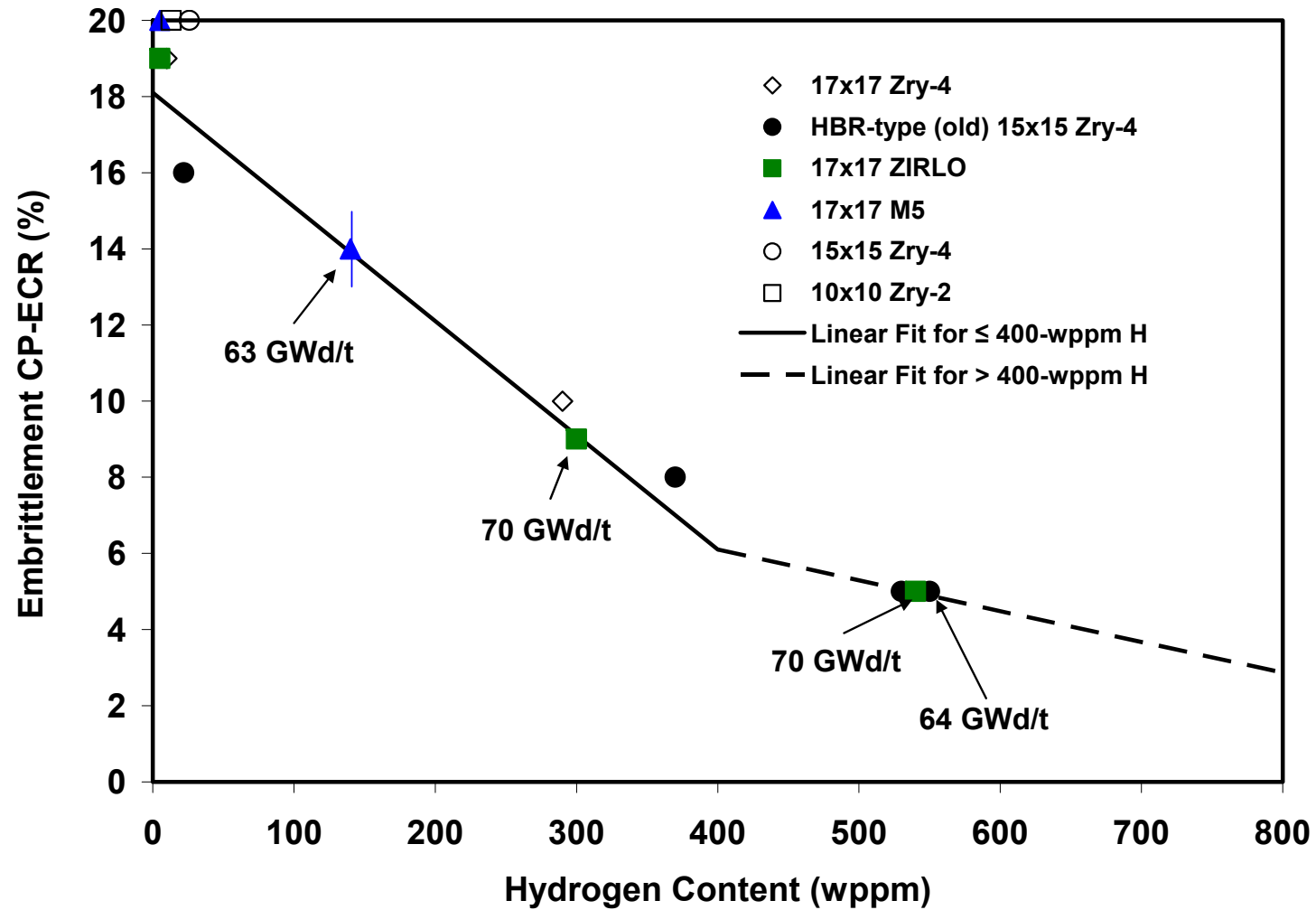


Fig. 7. Ductile-to-brittle transition oxidation level (CP-ECR) as a function of pre-test hydrogen content in cladding metal for as-fabricated (AF), prehydrided (PF), and high-burnup cladding materials. Samples were oxidized at $\leq 1200^\circ\text{C}$ and quenched at 800°C . For cladding materials with about 550-wppm hydrogen, embrittlement occurred for peak oxidation temperatures of 1160 - 1190°C .

The data trend in Fig. 7 can be represented by a higher-order function or by a bi-linear function. The bi-linear function shown in Fig. 7 was derived in the following way. Data points between 140 and 360 wppm were used to determine the line corresponding to ≤ 400 -wppm hydrogen. Data points for high-burnup M5 and ZIRLO were assigned a weighting factor of two, while data for prehydrided Zry-4 were given a weighting factor of one. Although the data of $< 8\%$ CP-ECR at 340-wppm hydrogen is not shown in Fig. 7, the embrittlement threshold at 340 wppm was assumed to be 7% and weighted with a factor of 2 to derive the linear fit. This is a more reasonable approach than to constrain the line to be below 8% at 340-wppm hydrogen, which would give this single point too much weight. A similar approach was used to fit the data at $> 400^\circ\text{C}$: the high-burnup Zry-4 and ZIRLO data were assigned a weighting factor of two, while the prehydrided Zry-4 data point was assigned a weighting factor of 1. Also, a continuity constraint was imposed to ensure that the two linear fits agreed at 400-wppm hydrogen. The resulting equations are:

$$\text{CP-ECR} = 18.1 - 0.030 C_H, \text{ for } C_H \leq 400 \text{ wppm H} \quad (2)$$

and

$$\text{CP-ECR} = 6.1 - 0.0078 (C_H - 400 \text{ wppm}), \text{ for } C_H > 400 \text{ wppm H} \quad (3)$$

where C_H is the pre-test hydrogen content in the cladding metal (in wppm) and CP-ECR is the oxidation level (in %). At 340-wppm hydrogen, the embrittlement CP-ECR from Eq. 2 is 7.9%.

If very rapid heating rates (e.g., 10-20°C/s) from 1000°C to 1200°C had been used in the experiments, it is probable that the shape of the embrittlement CP-ECR vs. hydrogen content would exhibit an increasing downward slope (convex shape). However, with the 2-3°C/s ramp rates used in the Argonne tests, which are more reasonable upper bounds for LOCA, embrittlement for higher-hydrogen samples occurs during the ramp from 1000°C to 1200°C. Because of this decrease in temperature with increasing hydrogen content, the shape of the embrittlement curve shown in Fig. 7 exhibits a decreasing downward slope (convex shape) as hydrogen content increases. To minimize the effects of ramp rate on the embrittlement threshold, it is recommended that future tests with prehydrided cladding be conducted at 1000-1100°C for hydrogen contents > 350 wppm for 17×17 cladding and > 500 wppm for thicker 15×15 cladding.

References

1. Michael Billone, Yong Yan, Tatiana Burtseva, and Robert Daum, "Cladding Embrittlement during Postulated Loss-of-Coolant Accidents," NUREG/CR-6967, July, 2008; available online in NRC ADAMS as ML082130389 at <http://www.nrc.gov/NRC/reading-rm/adams.html>.
2. "Procedure for Conducting Oxidation and Post-Quench Ductility Tests with Zirconium-based Cladding Alloys," Argonne National Laboratory, Mar. 31, 2009; available online in NRC ADAMS as ML090900841 at <http://www.nrc.gov/NRC/reading-rm/adams.html>.

Appendix A

Determination of Hydrogen Content in Metal of Irradiated and Corroded Cladding

The standard approach for determining the hydrogen content in irradiated cladding is to section a ring, weight the ring, heat the ring to melting, and measure the hydrogen evolved from the sample. For LOCA embrittlement, it is desirable to know the hydrogen content of the cladding metal. However, for the standard approach there are two sources of uncertainty, which have counter-balancing effects. The mass of the sample consists of the mass of the corrosion layer (M_C), the mass of the cladding metal (M_M) and the mass of the fuel-cladding bond (M_B). For higher-burnup cladding, the mass of the bond layer can be significant if the defueling process is poor. The total hydrogen evolved from the sample consists of hydrogen mass in the corrosion layer (H_C), in the cladding metal (H_M) and in the cladding bond (H_B). The bond layer can pick up hydrogen evolved from the nitric acid defueling process. Let L_H (in wppm) be the total hydrogen (H_S) evolved from the sample divided by the total mass of the sample (M_S). Equation A1 represents what is generally reported for the hydrogen content of the cladding:

$$L_H = (H_S / M_S) \times 10^6 = (H_C + H_M + H_B) / (M_C + M_M + M_B) \times 10^6 \quad (A1)$$

Based on Eq. A1, the hydrogen content in the cladding metal may be greater or less than what is measured for the irradiated sample. There are two approaches that can be used to improve the reported values for cladding metal hydrogen content. For the first approach, the total hydrogen in the cladding metal can be determined by means of two stage heating. LECO markets a hydrogen analyzer (Model RH600) that can be programmed for the two stage heating. The first stage is the lower temperature stage during which hydrogen in the corrosion and bond oxide layers is driven off. The second stage is the heating-to-melting phase during which hydrogen in the metal is driven off. The lower temperature can be determined by varying it until the hydrogen evolved in the second-stage heating is a constant. The data can be represented by Eq. A2.

$$L_{HM} = (H_M / M_S) \times 10^6 = H_M / (M_C + M_M + M_B) \times 10^6 \quad (A2)$$

The second correction that needs to be made is to the cladding metal mass relative to the total sample mass. This can be made by measuring the total mass of a ≥ 25 -mm-long sample to determine the sample mass per unit length (M_S/L) and by measuring the sample outer diameter (standard profilometry), the corrosion layer thickness (eddy current or metallography) and the cladding metal wall thickness (metallography). From the measurements, the cladding outer- and inner-diameter can be determined, as well as the cladding metal mass per unit length (M_M/L). Let the metal mass correction factor be defined as $f_{MM} = (M_S/L)/(M_M/L)$. Applying this correction factor to L_{HM} from Eq. 2 gives the hydrogen content in the cladding metal (C_{HM} in wppm):

$$C_{HM} = f_{MM} \times (H_M / M_S) \times 10^6 \quad (A3)$$

Based on Argonne experience, the metal mass correction factor is in the range of 1.06 to 1.10 for high-burnup ZIRLO with corrosion layer thicknesses of about 25-45 μm . The factors do not scale directly with the corrosion layer thickness because the mass of the fuel-cladding bond varies from defueled segment to defueled segment. For high-burnup M5 with a corrosion layer in the range of 10-15 μm , the factor can vary from 1.003 to 1.06, where the low value is for a segment whose inner-surface was wire brushed.

Given the magnitude of the cladding metal mass correction factor, it is not accurate to subtract the hydrogen content of the corrosion layer without accounting for the mass correction factor.

Argonne used a slightly different method for determining the hydrogen content in the cladding metal. The LECO machine was used to measure the pre-test hydrogen content of short rings adjacent to locations from which LOCA test samples were sectioned. These measurements give L_{HM} as defined by Eq. A1. For most of the LOCA oxidation samples, the pre $[(M)_i]$ - and post $[(M)_{POX}]$ -test weights of the samples were measured, along with the pre-test length of the sample. Thus, the pre-test mass per unit length could be determined, along with the LOCA sample weight gain. LECO hydrogen measurements were performed after the LOCA oxidation and/or after ring-compression tests. Generally, the sample mass was larger than the pre-test sample mass. This was due to the higher availability of post-test material. The larger post-test mass increased the reliability of the data.

A two-step process was used to determine the pre-test hydrogen content in the cladding metal. The post-oxidation LECO hydrogen measurements $[(L_H)_{POX}$ in wppm] were multiplied by the weight-gain factor $[f_{wg} = (M)_{POX}/(M)_i]$ to normalize the hydrogen content to the pre-test weight of the sample. The resulting hydrogen concentration was then multiplied by the same metal-mass correction factor (f_{MM}) defined previously. The equation used to calculate the pre-test hydrogen content in the metal is:

$$C_{HM} = f_{wg} \times f_{MM} \times (L_H)_{POX} \quad (A4)$$

Table A1 summarizes the results for the pre-test hydrogen content in the metal calculated from the measured post-oxidation hydrogen content and compares them to the pre-test values measured for the corroded cladding. For high-burnup M5 cladding with a corrosion layer of 10-15 μm (12 μm measured by metallography at one location), the average hydrogen content in the metal was 20 wppm higher than the hydrogen content measured for the corroded pre-test sample. This difference is not very significant in that bare, as-fabricated cladding tested in the Argonne program picked up as much as 20 wppm of hydrogen during oxidation at 1200°C. For high-burnup ZIRLO cladding with a corrosion layer of 25-30 μm (26 μm measured by metallography at one location), the average hydrogen content in the metal was 20 wppm less than the hydrogen content measured for the corroded pre-test sample. This difference is not significant relative to the circumferential and axial variations measured, as well as the differences in sample masses. For high-burnup ZIRLO cladding with a corrosion layer of 40-45 μm (41 and 43 μm measured by metallography at two locations), the average hydrogen content in the metal was 50 wppm less than the hydrogen content measured for the corroded pre-test sample. This difference may be significant. However, it is small relative to the circumferential and axial variations measured, as well as the effects of different sample masses for the two types of measurements.

For high-burnup H. B. Robinson (HBR) 15×15 Zry-4, pre-test hydrogen measurements at a location between LOCA oxidation samples, along with post-test hydrogen measurements were unreliable because the samples were inadequately defueled. An additional segment was sectioned from an axial location adjacent to the LOCA oxidation samples, carefully defueled and sectioned into 8 rings for hydrogen determination. The hydrogen content (550±100 wppm) was relatively constant from ring to ring. Also, the total mass of the rings was 1.52 g. Thus, the 550±100 wppm of hydrogen measured is a very reliable characterization of the pre-test hydrogen content of the corroded cladding. The corrosion layer was ≈70- μm thick and the cladding metal wall was 710- μm thick. Including the bond layer, the metal-mass correction factor was calculated to be 1.09. However, the corrosion layer had about 10% porosity and may have contained a significant amount of hydrogen. As no reliable post-oxidation hydrogen data are available for the HBR LOCA samples, it is assumed that the mass-correction factor and the corrosion-layer-hydrogen correction factor balance out to give 550±100 wppm of hydrogen in the cladding metal.

Table A1 Determination of Pre-test Cladding Metal Hydrogen Content based on Post-oxidation Hydrogen Measurements for High-burnup M5 and ZIRLO Samples used for LOCA Post-quench Ductility Determination; f_{wg} = post-test-weight/pre-test-weight, f_{MM} = pre-test sample-mass/metal-mass

Material	Test # (ID#)	$(L_H)_{POX}$, wppm (mass)	f_{wg}	Pre-test mass/L g/cm	f_{MM}	Pre-test H in Clad. Metal, wppm	Pre-test H in Corroded Cladding, wppm (mass)
M5	MI#1 (645A1)	85±7 (0.35 g)	1.040	1.036	1.028	91±8	101±21 (0.1 g)
	MI#2 (645A4)	107±14 (0.38 g)	1.040	1.042	1.035	115±15	101±21 (0.1 g)
	MI#4 (645B6)	109±9 (0.26 g)	1.052	1.066	1.059	122±10	108±5 (0.22 g)
	MI#5 (645B2)	130±11 (0.33 g)	1.047	1.039	1.033	140±12	108±5 (0.22 g)
	MI#6 (645C3)	138±15 (0.25 g)	1.047	1.044	1.025	147±14	108±10 (0.40 g)
	MI#7 (645C6)	130±15 (1.31 g)	1.039	1.007	1.003	135±15	108±10 (0.40 g)
ZIRLO	ZLI#4 (648F2)	505±107 (0.26)	0.996	1.074	1.074	540±114	620±140 (0.55 g)
	ZLI#5 (648F6)	505±107 (0.27)	0.99	1.074	1.096	592±115	600±150 (0.36 g)
	ZLI#6 (648E2)	414±115 (0.79)	1.004	1.073	1.080	448±104	500±120 (0.24 g)
	ZLI#7 (648B2)	316±31 (0.28)	1.011	1.068	1.062	340±34	366±30 (0.41 g)
	ZLI#8 (648A3)	267±33 (0.76)	1.023	1.084	1.078	294±37	310±32 (0.53 g)
	ZLI#9 (648A6)	274±33 (0.72)	1.017	1.067	1.061	296±35	310±32 (0.53 g)

Appendix B

Load-displacement Curves for New Tests with High-burnup ZIRLO Samples with Pre-test Hydrogen Contents of 300-340 wppm in the Cladding Metal

Figures B1-B9 show the load-displacement curves for rings sectioned from LOCA samples used in tests ZLI#7-9 and ZLI#11. Test conditions are listed on the graphs.

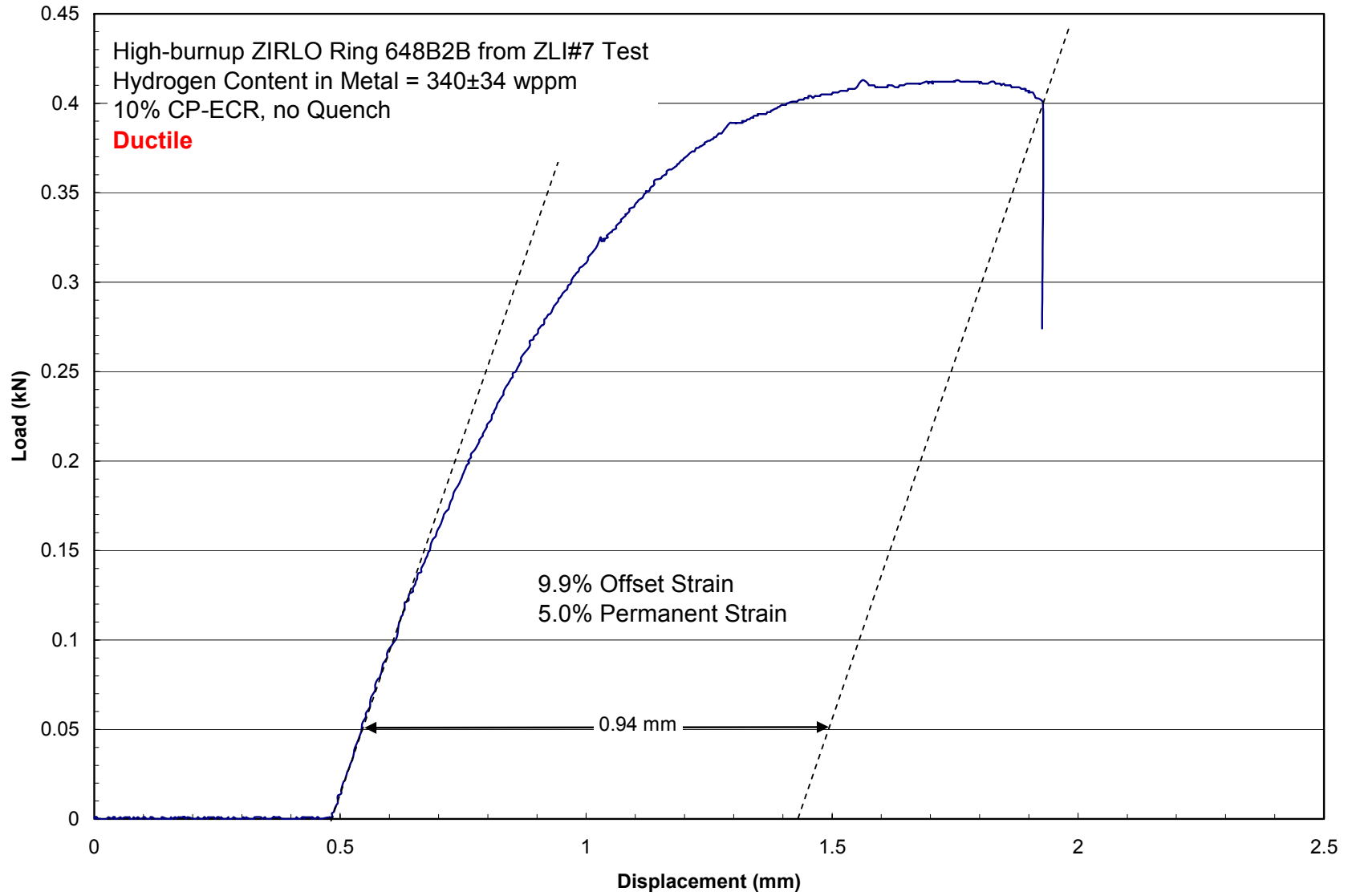


Fig. B1. Load-displacement curve for high-burnup ZIRLO cladding oxidized to 10% CP-ECR and cooled without quench: Ring 648B2B.

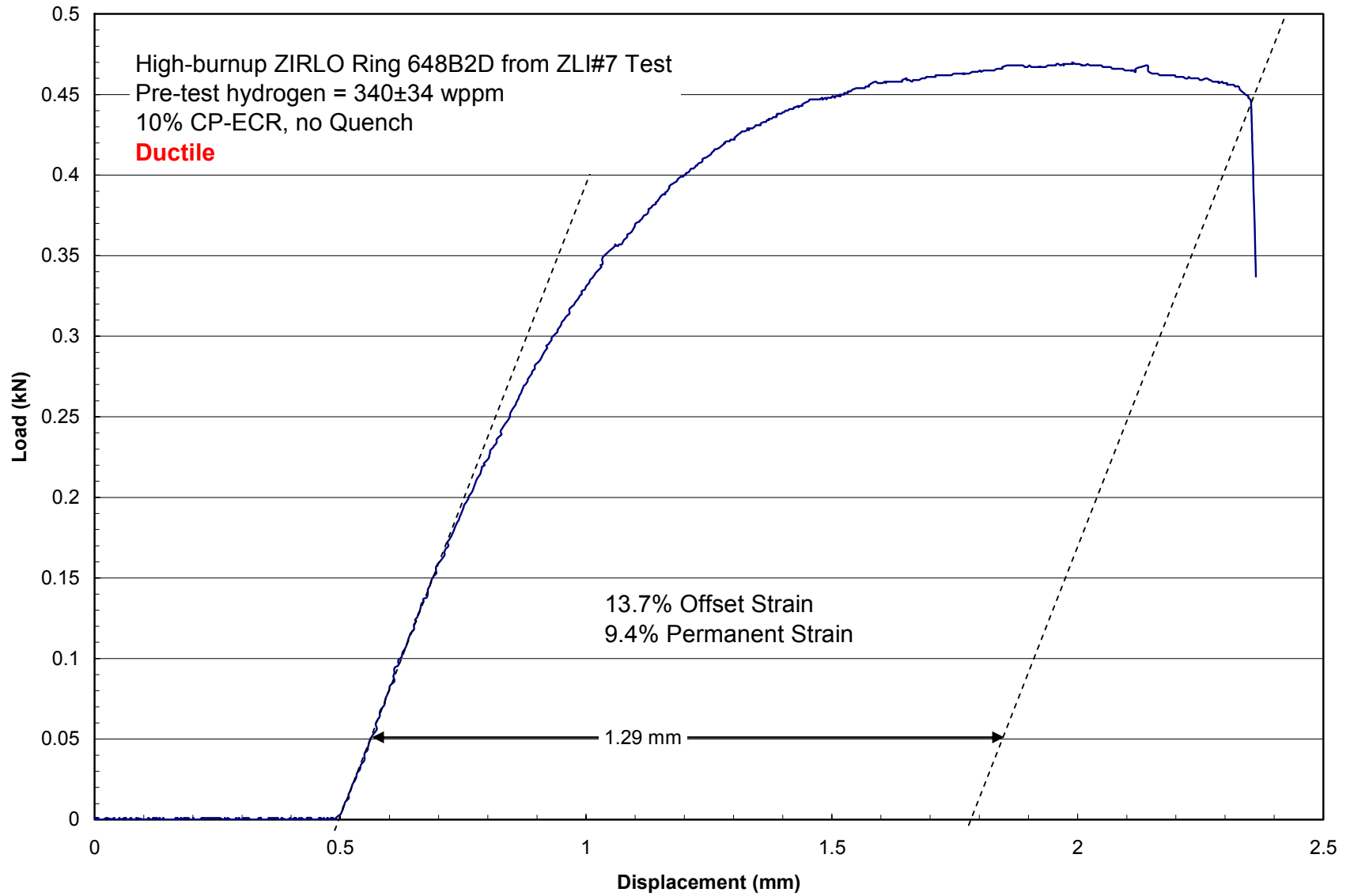


Fig. B2. Load-displacement curve for high-burnup ZIRLO cladding oxidized to 10% CP-ECR and cooled without quench: Ring 648B2D.

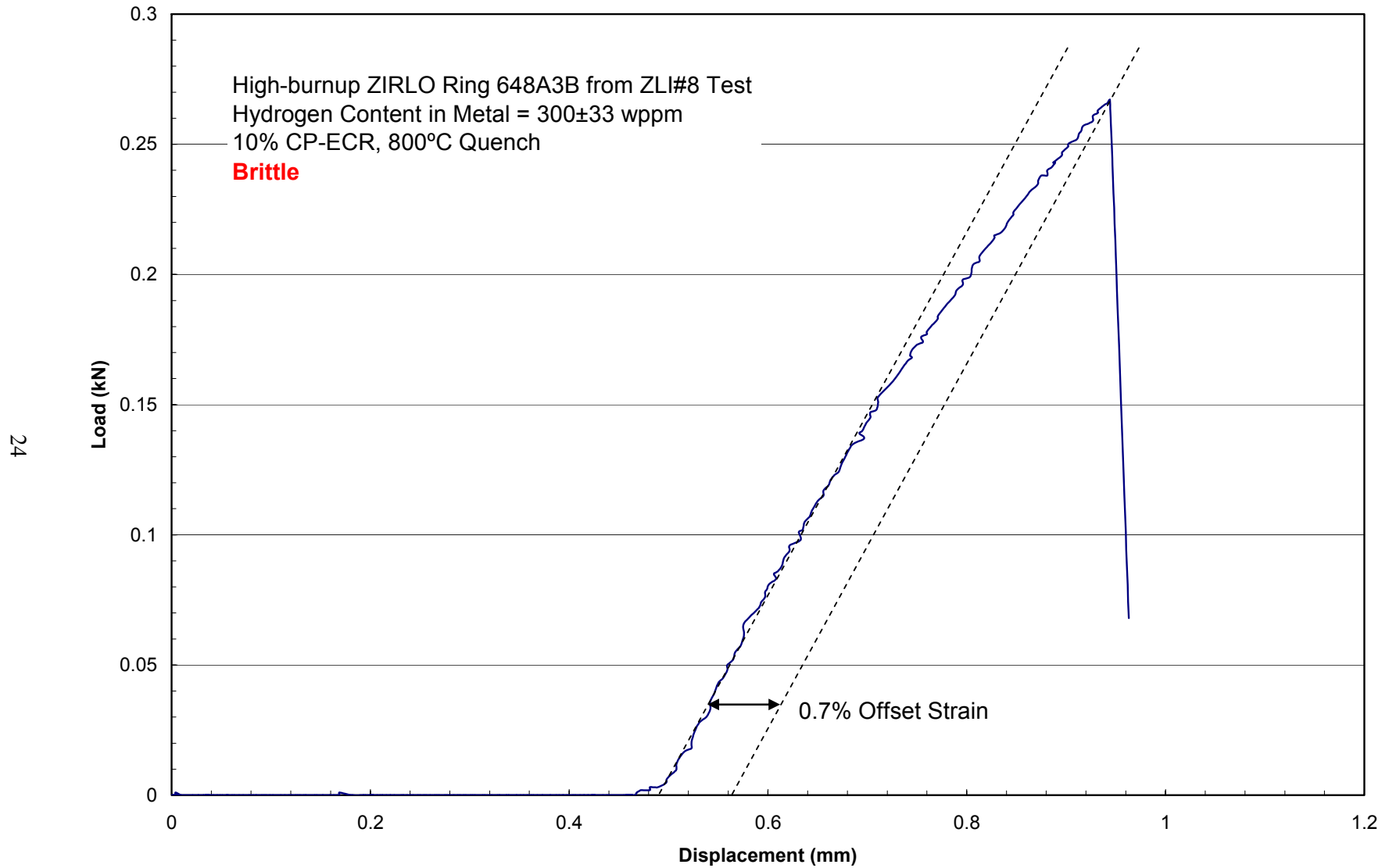


Fig. B3. Load-displacement curve for high-burnup ZIRLO cladding oxidized to 10% CP-ECR and quenched at 800°C: Ring 648A3B.

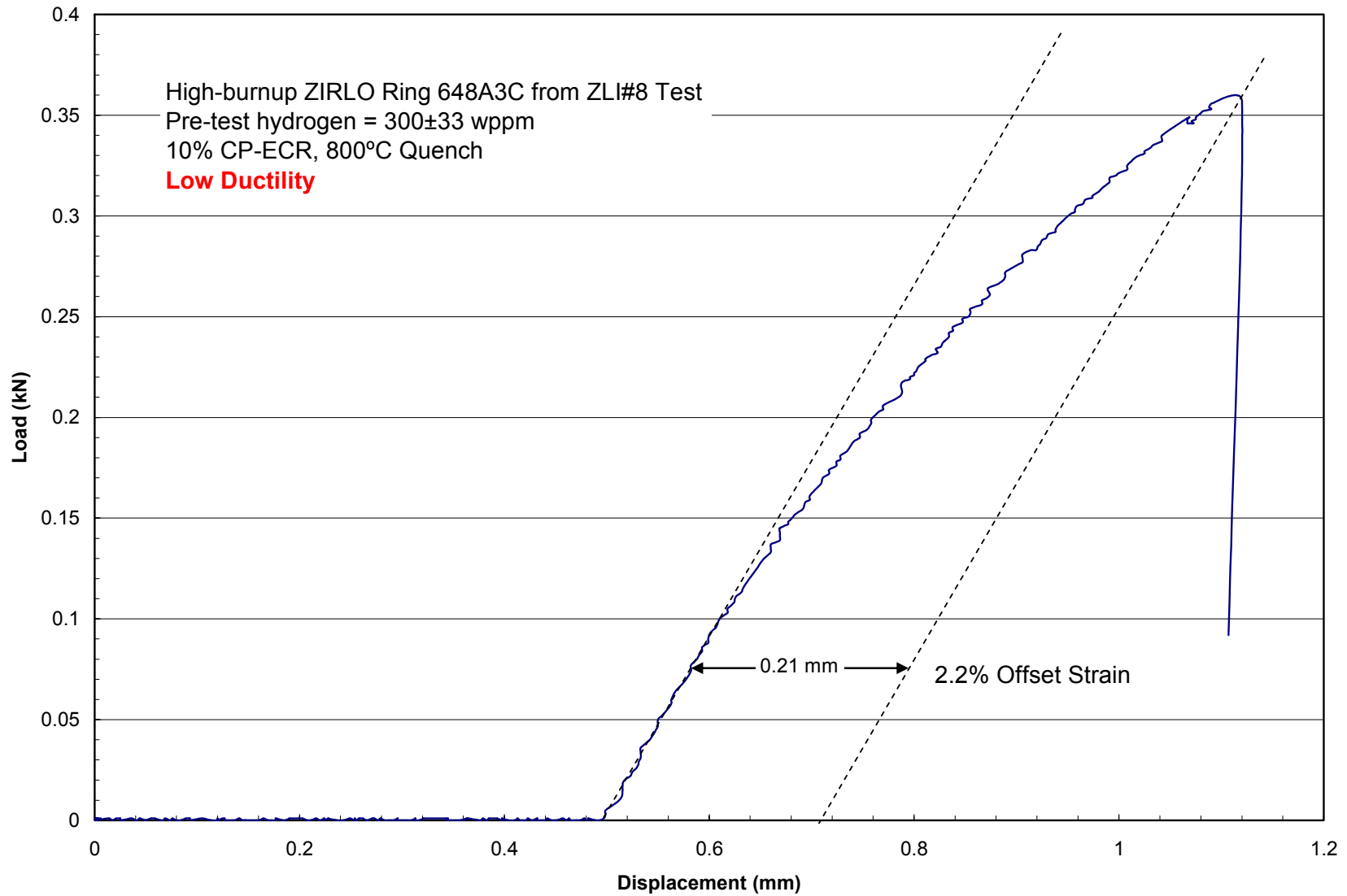


Fig. B4. Load-displacement curve for high-burnup ZIRLO cladding oxidized to 10% CP-ECR and quenched at 800°C: Ring 648A3C.

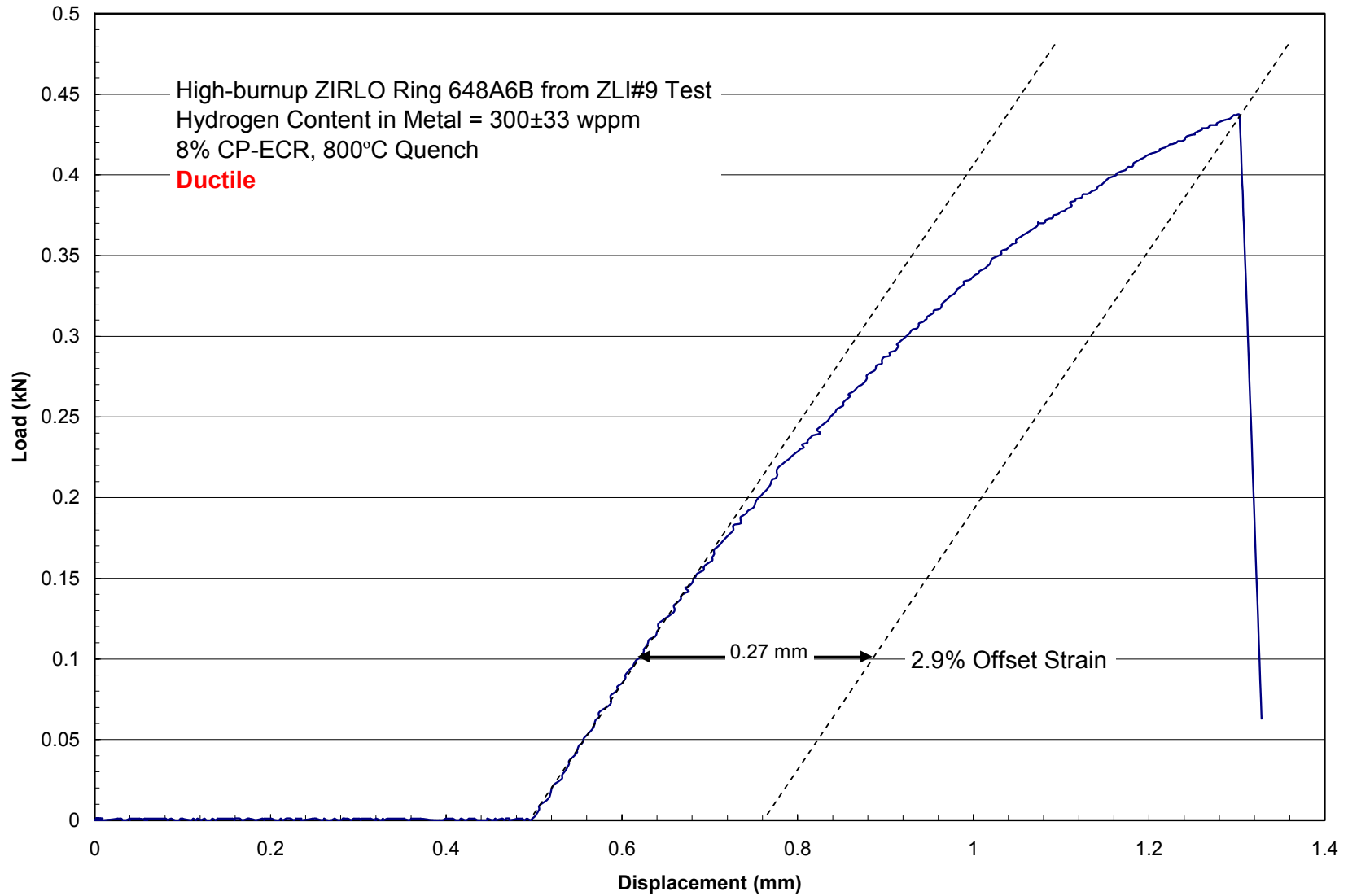


Fig. B5. Load-displacement curve for high-burnup ZIRLO cladding oxidized to 8% CP-ECR and quenched at 800°C: Ring 648A6B.

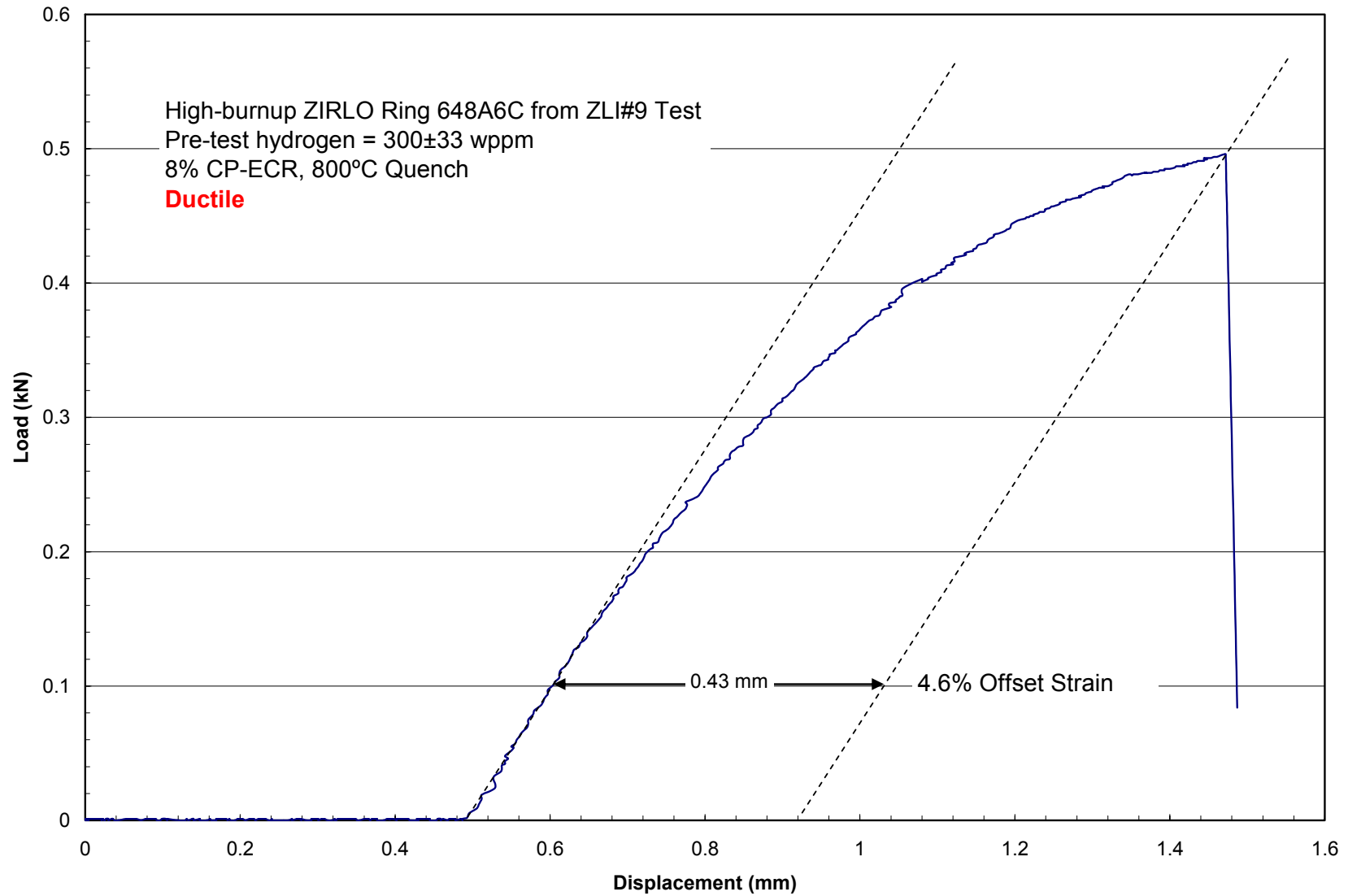


Fig. B6. Load-displacement curve for high-burnup ZIRLO cladding oxidized to 8% CP-ECR and quenched at 800°C: Ring 648A6C.

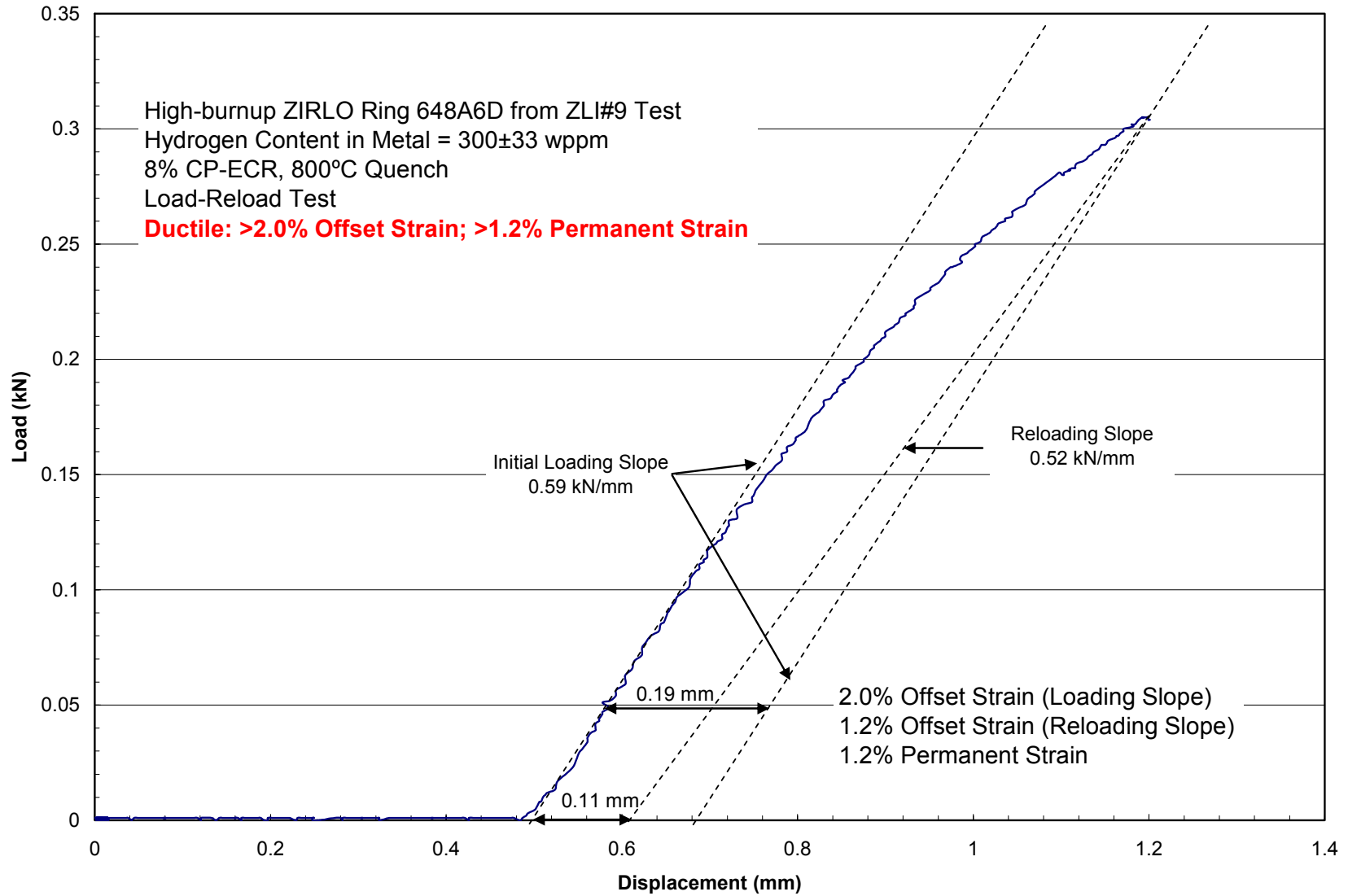


Fig. B7. Load-displacement curve for high-burnup ZIRLO cladding oxidized to 8% CP-ECR and quenched at 800°C: Ring 648A6D.

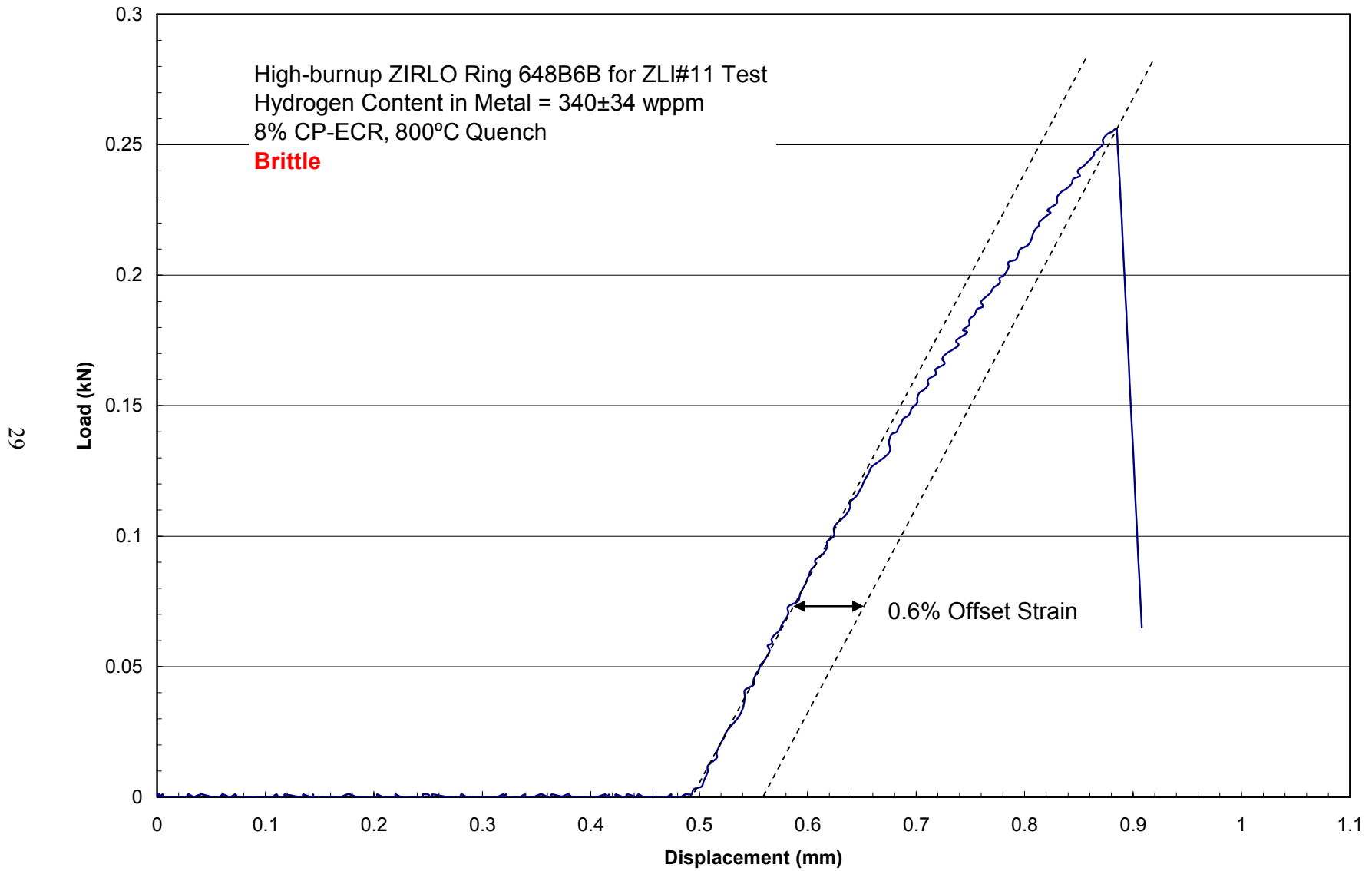


Fig. B8. Load-displacement curve for high-burnup ZIRLO cladding oxidized to 8% CP-ECR and quenched at 800°C: Ring 648B6B.

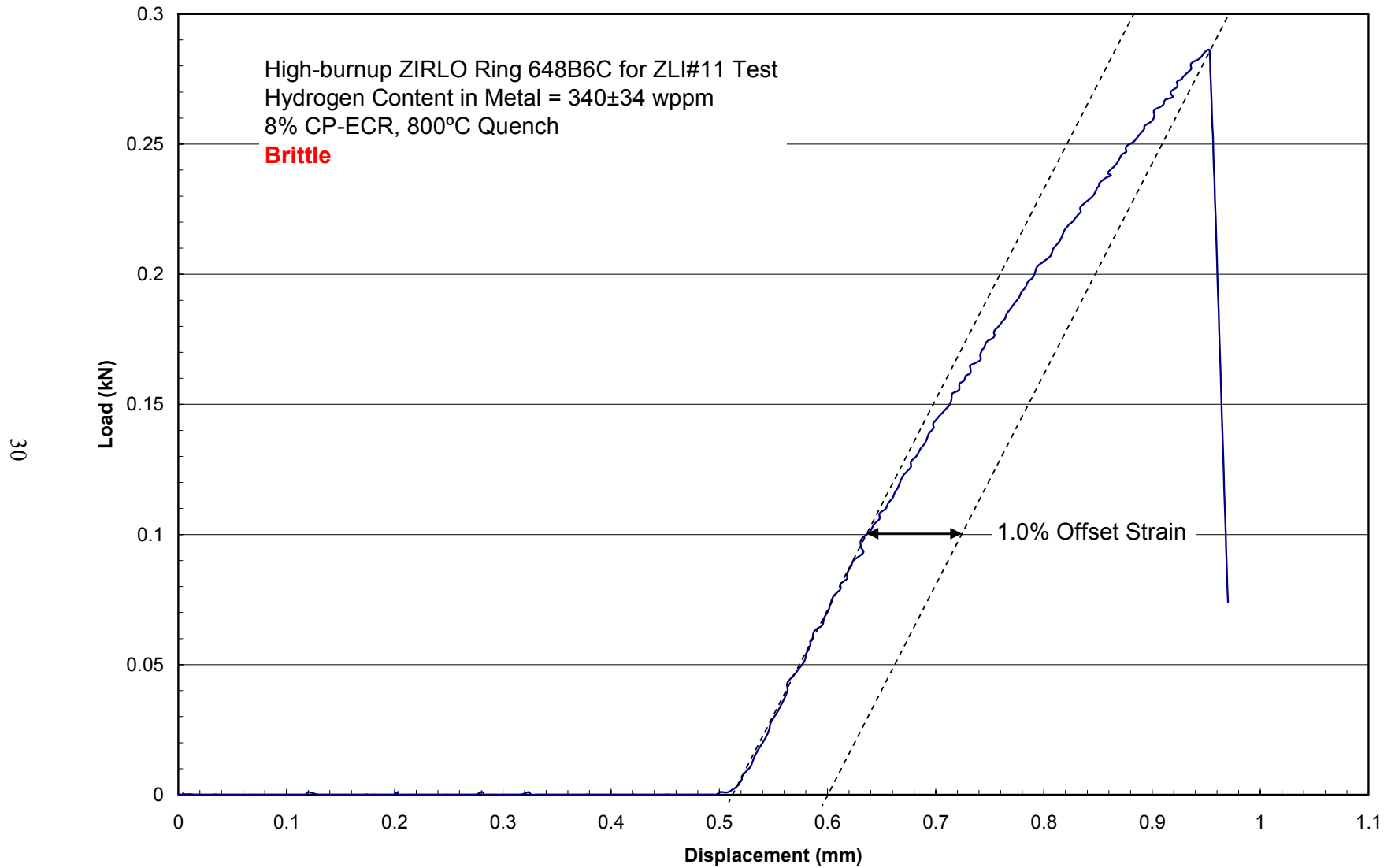


Fig. B9. Load-displacement curve for high-burnup ZIRLO cladding oxidized to 8% CP-ECR and quenched at 800°C: Ring 648B6C.